

Properties of broadband depth-graded multilayer mirrors for EUV optical systems

A. E. Yakshin^{1*}, I. V. Kozhevnikov², E. Zoethout¹, E. Louis¹, and F. Bijkerk^{1,3}

¹FOM-Institute for Plasma Physics Rijnhuizen, NL-3430 BE Nieuwegein, The Netherlands

²Institute of Crystallography, Leninsky prospect 59, Moscow 119333, Russia

³also at MESA + Institute for Nanotechnology, University of Twente, The Netherlands

*yakshin@rijnhuizen.nl

Abstract: The optical properties of a-periodic, depth-graded multilayer mirrors operating at 13.5 nm wavelength are investigated using different compositions and designs to provide a constant reflectivity over an essentially wider angular range than periodic multilayers. A reflectivity of up to about 60% is achieved in these calculation in the $[0, 18^\circ]$ range of the angle of incidence for the structures without roughness. The effects of different physical and technological factors (interfacial roughness, natural interlayers, number of bi-layers, minimum layer thickness, inaccuracy of optical constants, and thickness errors) are discussed. The results from an experiment on the fabrication of a depth-graded Mo/Si multilayer mirror with a wide angular bandpass in the $[0, 16^\circ]$ range are presented and analyzed.

©2010 Optical Society of America

OCIS codes: (230.0230) Optical devices; (230.4170) Multilayers; (310.0310) Thin films; (310.4165) Multilayer design; (340.0340) X-ray optics; (340.7480) X-rays, soft x-rays, extreme ultraviolet (EUV);

References and links

1. D. A. Tichenor, A. K. Ray-Chaudhuri, S. H. Lee, H. N. Chapman, W. C. Replogle, K. W. Berger, R. H. Stulen, G. D. Kubiak, L. E. Klebanoff, J. B. Wronosky, D. J. O'Connell, A. H. Leung, K. L. Jefferson, W. P. Ballard, L. C. Hale, K. Blaedel, J. S. Taylor, J. A. Folta, E. Spiller, R. Soufii, G. E. Sommargren, D. W. Sweeney, P. Naulleau, K. A. Goldberg, E. M. Gullikson, J. Bokor, D. T. Attwood, U. Mickan, R. Hansen, E. Panning, P.-Y. Yan, J. E. Bjorkholm, and C. W. Gwyn, "Initial Results from the EUV Engineering Test Stand," *Proc. SPIE* **4506**, 9 (2001).
2. H. Meiling, J. Benschop, U. Dinger, and P. Kurz, "Progress of the EUVL alphasource," *Proc. SPIE* **4343**, 38–50 (2001).
3. P. Lee, "Uniform and graded multilayers as x-ray optical elements," *Appl. Opt.* **22**(8), 1241–1246 (1983).
4. K. D. Joensen, P. Voutov, A. Szentgyorgyi, J. Roll, P. Gorenstein, P. Hoghoj, and F. E. Christensen, "Design of grazing-incidence multilayer supermirrors for hard-x-ray reflectors," *Appl. Opt.* **34**(34), 7935–7944 (1995).
5. P. van Loevezijn, R. Schlatmann, J. Verhoeven, B. A. van Tiggelen, and E. M. Gullikson, "Numerical and experimental study of disordered multilayers for broadband X-ray reflection," *Appl. Opt.* **35**(19), 3614–3619 (1996).
6. V. V. Protopopov, and V. A. Kalnov, "X-ray multilayer mirrors with an extended angular range," *Opt. Commun.* **158**(1-6), 127–140 (1998).
7. A. V. Vinogradov, and R. M. Faschenko, "An approach to the theory of X-ray multilayers with graded period," *Nucl. Instrum. Methods Phys. Res. A* **448**(1-2), 142–146 (2000).
8. Z. Wang, and A. G. Michette, "Optimization of depth-graded multilayer designs for EUV and X-ray optics," *Proc. SPIE* **4145**, 243–253 (2001).
9. I. Vkozhevnikov, I. Nbukreeva, and E. Ziegler, "Design of x-ray supermirrors," *Nucl. Instrum. Methods Phys. Res. A* **460**(2-3), 424–443 (2001).
10. K. D. Joensen, P. Gorenstein, F. E. Christensen, P. Høghøj, E. Ziegler, J. Susini, A. Freund, and J. Wood, "Multilayer mirrors: broad-band reflection coatings for the 15 to 100 keV range," *Proc. SPIE* **2253**, 299–308 (1994).
11. S. P. Vernon, D. G. Stearns, and R. S. Rosen, "Chirped multilayer coatings for increased x-ray throughput," *Opt. Lett.* **18**(9), 672–674 (1993).
12. C. Morawe, E. Ziegler, J.-C. Peffen, and I. V. Kozhevnikov, "Design and fabrication of depth-graded x-ray multilayers," *Nucl. Instrum. Methods Phys. Res. A* **493**(3), 189–198 (2002).
13. T. Feigl, S. Yulin, N. Benoit, and N. Kaiser, "EUV multilayer optics," *Microelectron. Eng.* **83**(4-9), 703–706 (2006).

14. T. Kuhlmann, S. A. Yulin, T. Feigl, N. Kaiser, H. Bernitzki, and H. Lauth, "Design and fabrication of broadband EUV multilayer mirrors," *Proc. SPIE* **4688**, 509 (2002).
15. S. Yulin, T. Kuhlmann, T. Feigl, and N. Kaiser, "Spectral reflectance tuning of EUV mirrors for metrology applications," *Proc. SPIE* **5037**, 286–293 (2003).
16. J. E. Dennis, Jr., and R. B. Schnabel, in *Numerical Methods for Unconstrained Optimization and Nonlinear Equations*, Prentice-Hall, Englewood Cliffs, ed. (NJ, 1983).
17. J. M. Slaughter, A. Shapiro, P. A. Kearney, and C. M. Falco, "Growth of molybdenum on silicon: Structure and interface formation," *Phys. Rev. B* **44**(8), 3854–3863 (1991).
18. A. E. Yakshin, E. Louis, P. C. Gorts, E. L. G. Maas, and F. Bijkerk, "Determination of the layered structure in Mo/Si multilayers by grazing incidence X-ray reflectometry," *Physica B* **283**(1-3), 143–148 (2000).
19. S. Bajt, D. G. Stearns, and P. A. Kearney, "Investigation of the amorphous-to-crystalline transition in Mo/Si multilayers," *J. Appl. Phys.* **90**(2), 1017–1025 (2001).
20. D. G. Stearns, R. S. Rosen, and S. P. Vernon, "Fabrication of high-reflectance Mo-Si multilayer mirrors by planar-magnetron sputtering," *J. Vac. Sci. Technol. A* **9**(5), 2662–2669 (1991).
21. S. Yulin, T. Feigl, T. Kuhlmann, N. Kaiser, A. I. Fedorenko, V. V. Kondratenko, O. V. Poltseva, V. A. Sevryukova, A. Yu. Zolotaryov, and E. N. Zubarev, "Interlayer transition zones in Mo/Si superlattices," *J. Appl. Phys.* **92**(3), 1216–1220 (2002).
22. S. Braun, H. Mai, M. Moss, R. Scholz, and A. Leson, "Mo/Si Multilayers with Different Barrier Layers for Applications as Extreme Ultraviolet Mirrors," *Jpn. J. Appl. Phys.* **41**(Part 1, No. 6B), 4074–4081 (2002).
23. N. Kaiser, S. Yulin, and T. Feigl, "Si-based multilayers with high thermal stability," *Proc. SPIE* **4146**, 91 (2000).
24. J. B. Shellan, P. Agmon, P. Yeh, and A. Yariv, "Statistical analysis of Bragg reflectors," *J. Opt. Soc. Am.* **68**(1), 18–27 (1978).
25. E. Spiller, "Characterization of Multilayer Coatings by X-Ray Reflection," *Rev. Phys. Appl. (Paris)* **23**(10), 1687–1700 (1988).
26. M. J. H. Kessels, F. Bijkerk, F. D. Tichelaar, and J. Verhoeven, "Determination of in-depth density profiles of multilayer structures," *J. Appl. Phys.* **97**(9 Issue 9), 093513 (2005).
27. I. Nedelcu, R. W. E. van de Kruijs, A. E. Yakshin, and F. Bijkerk, "Temperature-dependent nanocrystal formation in Mo/Si multilayers," *Phys. Rev. B* **76**(24 Issue 24), 245404 (2007).
28. I. Nedelcu, R. W. E. van de Kruijs, A. E. Yakshin, and F. Bijkerk, "Thermally enhanced interdiffusion in Mo/Si multilayers," *J. Appl. Phys.* **103**(8 Issue 8), 083549 (2008).
29. E. Louis, H.-J. Voorma, N. B. Koster, L. Shmaenok, F. Bijkerk, R. Schlattmann, J. Verhoeven, Yu. Ya. Platonov, G. E. van Dorssen, and H. A. Padmore, "Enhancement of reflectivity of multilayer mirrors for soft x-ray projection lithography by temperature optimization and ion bombardment," *Microelectron. Eng.* **23**(1-4), 215–218 (1994).
30. E. Spiller, in *Soft X-ray optics*, Bellingham ed. (SPIE Optical Engineering Press, Washington 1994).
31. R. Schlattmann, S. Lu, J. Verhoeven, E. J. Puik, and M. J. van der Wiel, "Modification by Ar and Kr ion bombardment of Mo/Si x-ray multilayers," *Appl. Surf. Sci.* **78**(2), 147–157 (1994).
32. J. Tümmler, H. Blume, G. Brandt, J. Eden, B. Meyer, H. Scherr, F. Scholz, and G. Ulm, "Characterization of the PTB EUV reflectometry facility for large EUVL optical components," *Proc. SPIE* **5037**, 265–273 (2003).
33. A. Gottwald, U. Kroth, M. Letz, H. Schoeppe, and M. Richter, "High-accuracy VUV reflectometry at selectable sample temperatures," *Proc. SPIE* **5538**, 157–164 (2004).

1. Introduction

The development of normal incidence multilayer mirrors has opened up new opportunities in the production of high resolution imaging optics for the extreme ultra-violet (EUV) and soft x-ray spectral regions. The development of multilayer-based optical systems for EUV photolithography, which provides nanometer resolution in the image plane [1,2], is representing a major technological and physics boost to this field.

However, the interferential nature of reflection from multilayer mirrors results in a narrow spectral and angular bandpass. This limits some of the applications for multilayer optics. For example, the angular bandpass of reflection is about 9° for a periodic Mo/Si mirror at $\lambda = 13.5$ nm (see Fig. 1, curve 1). However, future large aperture EUV-optical systems, which have diffraction limited resolution, will have radiation incident on the mirror at a range of angles that may exceed the bandpass of reflection. Evidently, a variation in the incidence angle φ_0 along a mirror surface (Fig. 2) can be compensated by a lateral variation in the period of a multilayer structure to obtain the Bragg condition of reflection at any point on a mirror surface. However, if the divergence of radiation $\delta\varphi$ (Fig. 2) exceeds the width of the Bragg peak, the only solution to the problem is to design a mirror that can provide a wider reflectivity bandpass with the required reflectivity profile. Strictly speaking such a design should also take into account the variation of phase. However the complex amplitude reflectivity profile can only be considered for a specific optical system, which is out of the

scope of this work. At the same time the factors influencing characteristics of such a system are the same as those considered in this work.

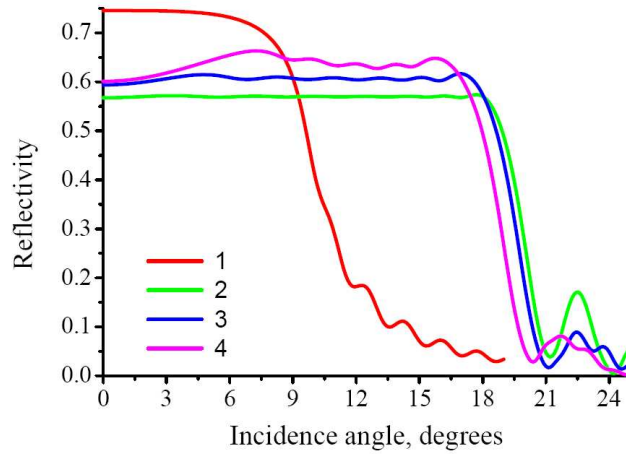


Fig. 1. The calculated reflectivity versus the angle of incidence of periodic (1) and depth-graded (2-4) Mo/Si multilayer mirrors for naturally polarized radiation at $\lambda = 13.5$ nm. The design of depth-graded mirrors was optimized to obtain the constant reflectivity R_0 in the $[0, 18^\circ]$ range of angle of incidence, the aimed value of R_0 being equal to 57% (2), 61% (3), and 70% (4). Calculations were performed for ideal multilayer structures without interlayers. The uppermost layer was silicon covered with naturally formed SiO_2 layer.

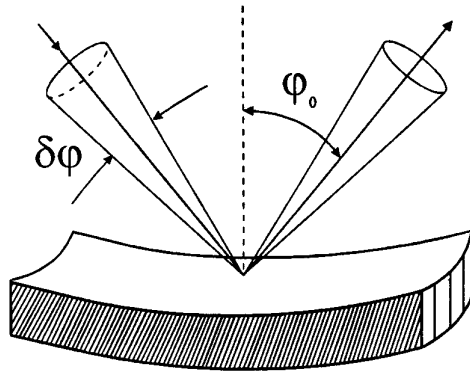


Fig. 2. Sketch of reflection of EUV radiation from a multilayer mirror.

The obvious way to widen the reflectivity bandpass of a multilayer mirror is to produce a gradual variation of the period with the depth of the multilayer structure stack [3]. An EUV beam, incident on such a structure over a range of angles will be reflected in accordance with the Bragg law, from different depths of the multilayer structure. Applying to the designing of depth-graded multilayer mirrors, the inverse problem can be formulated in the following manner. Suppose the angular, $R(\varphi)$, or the spectral, $R(\lambda)$, dependence of the reflectivity is a known function, one must find the required variation of the period and the Γ -ratio as a function of depth for the multilayer structure, $d(z)$ and $\Gamma(z)$, that will provide the given reflectivity profile $R(\varphi)$ or $R(\lambda)$.

Different theoretical approaches to this problem have been considered in [4–9]. Examples of wide bandpass multilayer mirrors, intended for operation in hard and soft x-ray spectral regions have been fabricated and tested, e.g., in [10–12] and [13–15], respectively. However, thorough study of the optical properties of the wideband EUV multilayer mirrors and factors limiting their ultimate parameters is still unavailable. Moreover, an optimum choice of

materials constituting a wideband EUV multilayer structure is not as evident as for the conventional periodic mirrors. This is caused by the fact that the optical response of the wideband multilayers is strongly deformed due to the interaction zones formed between the main pair of materials, while in the periodic multilayers these zones only reduce the overall reflectance.

This paper reports the results of theoretical analysis on determination of the optimum parameters for these structures, when constrained by requiring a constant reflectivity at a wavelength of 13.5 nm over a $[0, 18^\circ]$ range of angles of incidence. We will discuss the design, optimization, and approaches taken to increase the reflectivity of wider bandpass mirrors with a constant reflectivity profile, shown in Section 2. We consider the influence of different physical and technological factors on the reflectivity of depth-graded EUV multilayer mirrors in Section 3. Finally, we describe the fabrication and characteristics of a depth-graded Mo/Si multilayer mirror with a wider angular reflectivity bandpass in Section 4.

2. Wideband EUV multilayer mirrors with constant reflectivity

Our approach to the inverse problem of designing an EUV multilayer mirror with reflectivity, $R_0(\varphi)$, between the angles of incidence φ_{min} and φ_{max} (φ being the angle of incidence) is based on the minimization of the conventional merit function:

$$MF = \frac{1}{\varphi_{max} - \varphi_{min}} \int_{\varphi_{min}}^{\varphi_{max}} [R_0(\varphi) - R(\varphi)]^2 d\varphi \quad (1)$$

which characterizes the root-mean-square deviation of the calculated reflectivity profile $R(\varphi)$ from the intended reflectivity. The thicknesses of the deposited layers are considered as independent variables. The solution to the inverse problem is a set of layer thicknesses that provides a sufficiently deep minimum of the merit function of Eq. (1) so that the calculated reflectivity profile is close to the one aimed for. The studied multilayer mirrors are listed in Table 1.

We started our calculations with an ideal Mo/Si structure which had no interlayers between the adjacent materials and zero roughness (sample 1 in Table 1). The uppermost layer is a 2 nm SiO_2 oxide layer which results from the oxidation of the top silicon layer. The aim was to find a design that yielded a constant reflectivity ($R_0(\varphi) = R_0$) at wavelength $\lambda = 13.5$ nm over a $[0, 18^\circ]$ range of angles of incidence. Minimization of the merit function of Eq. (1) is performed using the conventional Levenberg-Marquardt algorithm [16].

The calculated reflectivity profiles (Fig. 1) show that if R_0 is considerably lower than the maximum possible reflectance for a periodic structure, the computational procedure obtains a very even reflectivity plateau (curve 2) over the given angular range. When R_0 is increased, the reflectivity profile becomes a varying function of the angle of incidence, which becomes stronger as R_0 is increased (compare the curves 3 and 4).

The calculated phase ψ of the amplitude reflectivity $r = |r| \cdot \exp(i\psi)$ is shown in Fig. 3 for the multilayer structures in Fig. 1. As seen, the phase variation of both periodic (curve 1) and depth-graded (curves 2-4) mirrors is similar, with the phase being a smooth and monotone function of the incidence angle in the angular range of high reflectance.

Table 1. Parameters of the depth-graded EUV multilayer mirrors ^a

Sample	Description	Number of bi-layers	Interlayers or barrier layers	<R> at RD = 0.6–0.7%	R_{int} , rad
1	$\text{SiO}_2/[\text{Si/Mo}]_N/\text{sub}$	100	none	61%	0.190
2	$\text{SiO}_2/[\text{Si/MoSi}_2/\text{Mo/MoSi}_2]_N/\text{sub}$	100	MoSi_2	54%	0.169
3	$\text{SiO}_2/[\text{Si/MoSi}_2/\text{Mo/MoSi}_2]_N/\text{sub}$	50	MoSi_2	52%	0.163
4	$\text{SiO}_2/[\text{Si/Mo}_2\text{C/Mo/Mo}_2\text{C}]_N/\text{sub}$	100	Mo_2C	58%	0.182
5	$\text{SiO}_2/[\text{Si/Mo}_2\text{C}]_N/\text{sub}$	100	none	56%	0.175

^a Parameters are optimized to provide constant reflectivity in the $[0, 18^\circ]$ range of the angle of incidence at $\lambda = 13.5$ nm. When calculating, we took the thickness of the SiO_2 oxide layer to be equal to 2 nm, and the thickness of the MoSi_2 interlayers or Mo_2C barrier layers to be equal to 1 nm. The substrate was fused silica.

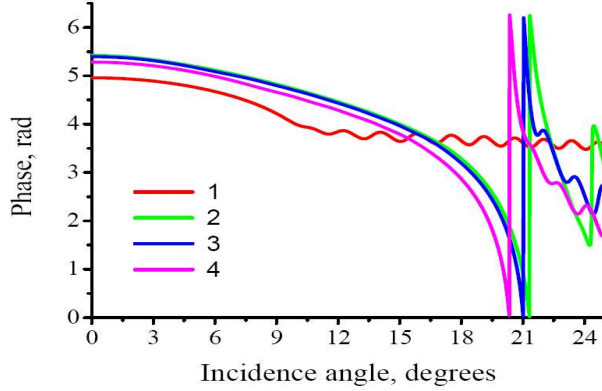


Fig. 3. The calculated phase of the amplitude reflectivity (s-polarized radiation) versus the angle of incidence for the multilayer mirrors in Fig. 1.

To characterize quantitatively the optical quality of a wideband multilayer mirror, we introduce the mean value of the reflectivity plateau, $\langle R \rangle$, and the relative dispersion of the reflectivity, RD , as follows:

$$\langle R \rangle = \frac{1}{\varphi_{\max} - \varphi_{\min}} \int_{\varphi_{\min}}^{\varphi_{\max}} R(\varphi) d\varphi \quad (2)$$

$$RD = \frac{1}{\langle R \rangle} \cdot \sqrt{\frac{1}{\varphi_{\max} - \varphi_{\min}} \int_{\varphi_{\min}}^{\varphi_{\max}} [R(\varphi) - \langle R \rangle]^2 d\varphi} \cdot 100\% \quad (3)$$

where $\varphi_{\min} = 0$ and $\varphi_{\max} = 18^\circ$. The relative dispersion of the reflectivity characterizes an undesirable deviation of the reflectivity curve from the flat plateau. The mean reflectivity versus the target value of the reflectivity plateau is shown in Fig. 4, curve 1. With increasing R_0 , the mean reflectivity differs from R_0 and tends to a certain value determined by the absorption of radiation in the material. The relative dispersion of the reflectivity versus the mean reflectivity is shown in Fig. 5, curve 1. It increases quickly with increasing $\langle R \rangle$, limiting the practicable value of the reflectivity plateau. If it is assumed that an acceptable level of the reflectivity dispersion is 0.6 – 0.7%, then the mean reflectivity is about 61%. The corresponding reflectivity profile is presented in Fig. 6, curve 1, and the variation of the layer thickness along the depth of Mo/Si multilayer mirror is shown in Fig. 7. Note that the inverse problem has typically a great number of solutions (minima of the merit function (1) of different depth), each of which results in different thickness profiles (see, e.g [9]).

By trying different initial thickness profiles, we found that the optimization procedure resulted in the small RD value and in depth-distributions that have a relatively smooth form, which also tend to be quasi-periodic in contrast to designs obtained in [14,15]. This is essential for the fabrication process, since smoother profiles are considered to be easier to implement due to more accurate calibration of the layer thicknesses for commonly used deposition techniques.

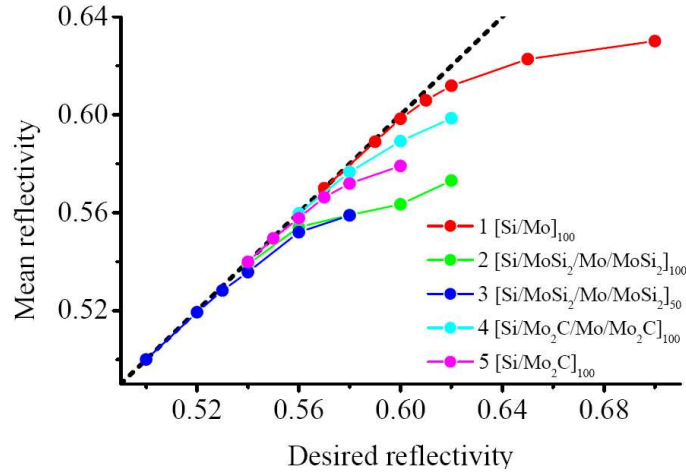


Fig. 4. The mean reflectivity $\langle R \rangle$ of depth-graded multilayer mirrors in the $[0, 18^\circ]$ range of angle of incidence versus the aimed reflectivity plateau R_0 . The curve number in the figure corresponds to the number of a structure in Table 1. The dashed straight line corresponds to the ideal case $\langle R \rangle = R_0$.

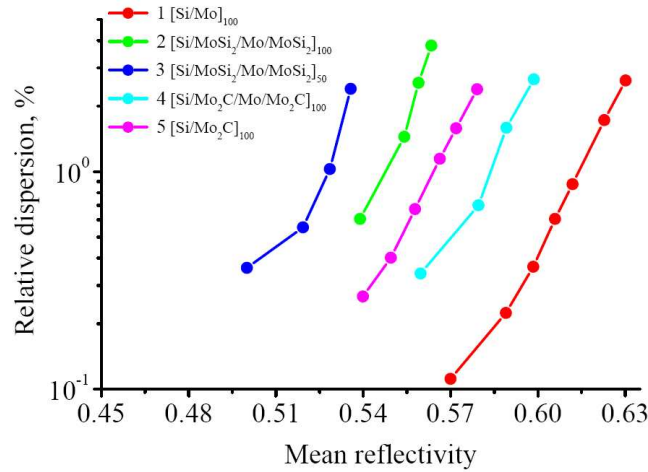


Fig. 5. The relative dispersion of reflectivity of depth-graded multilayer mirrors in the $[0, 18^\circ]$ range of angle of incidence versus the mean reflectivity value. The curve number in the figure corresponds to the structure number in Table 1.

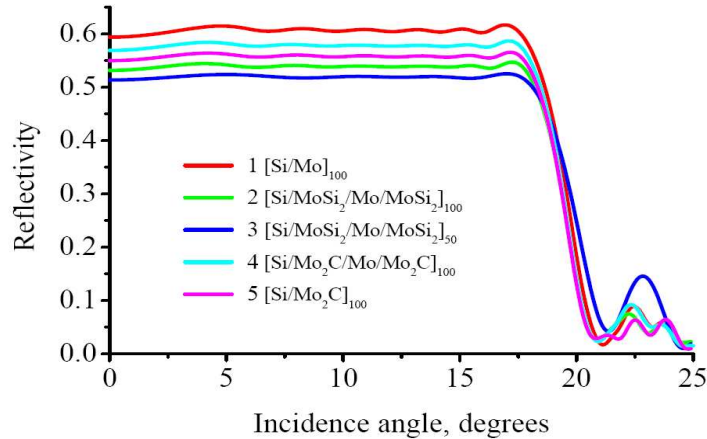


Fig. 6. The reflectivity of the studied depth-graded multilayer mirrors at about the same relative dispersion of the reflectivity $RD \sim 0.6\text{--}0.7\%$. Curve number in the figures corresponds to the structure number in Table 1.

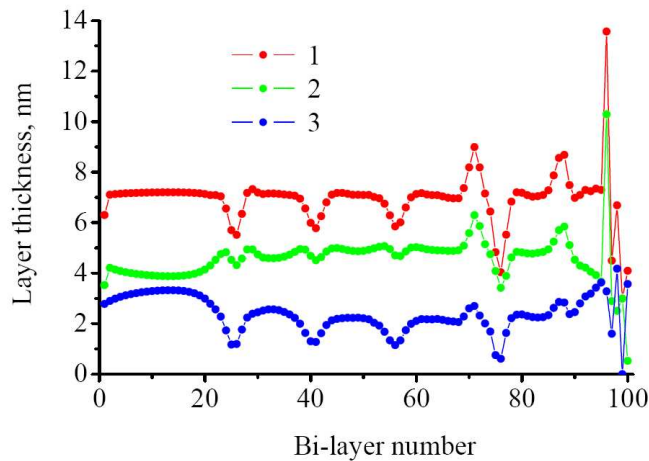


Fig. 7. The depth-distribution of the period (beginning from the top) (1) as well as the thickness of the Si (2) and Mo (3) layers for the Mo/Si multilayer mirror (sample 1 in Table 1) optimized for the constant reflectivity $R_0 = 61\%$ at $\lambda = 13.5$ nm in the $[0, 18^\circ]$ range of the angle of incidence.

One more parameter characterizing optical properties of a wideband multilayer mirror is the integral reflectivity R_{int} , i.e. the reflectivity integrated over the $[0, 18^\circ]$ angular interval. The values of R_{int} of the studied mirrors are presented in Table 1. The R_{int} for a depth-graded Mo/Si multilayer mirror based on an ideal stack (sample 1 in Table 1) is equal to 0.190 rad that is about 1.33 times higher compared to that of a periodic multilayer mirror based on an ideal stack ($R_{\text{int}} = 0.143$ rad). We would like to note that the integral reflectivity can be further increased by performing a special optimization of a multilayer structure to provide the maximal value of R_{int} . However, in this case the reflectivity will become strongly oscillating function of the incidence angle. Finding a compromise solution between the flatness of the reflectivity profile and integral reflectivity acceptable for a specific optical system is out of the scope of this paper. At the same time the factors influencing characteristics of such systems in general are the same as those considered in this work for achieving flat reflectivity profile.

In general, for multilayer structures, the flat reflectivity profile cannot be achieved using designs based on an ideal stack. In the Mo/Si system, the formation of natural interlayers will

considerably alter the reflectivity, therefore these interlayers have to be taken into account in the design process. In the next step we study the influence of this effect, including experimentally estimated parameters for the interlayers.

The interlayers of different silicides and thicknesses have been identified between Mo and Si layers depending on the deposition method and measurement technique [17–22]. For our estimate, we approximate the interlayers by introducing 1 nm MoSi₂ interlayers at every boundary. Using this approach, the only variables in the merit function are still the thicknesses of the Mo and Si layers. The mean reflectivity versus the aimed value of the reflectivity plateau is shown in Fig. 4 (curve 2), and the relative dispersion of the reflectivity versus the mean reflectivity is shown in Fig. 5 (curve 2). The calculated reflectivity profile for this structure is presented in Fig. 6 (curve 2). Essentially, the interlayers result in a decrease in the mean reflectivity compared to an ideal structure with the same dispersion of the reflectivity. For example, when *RD* is ~0.6–0.7%, the loss is about 7%. Note that the loss due to the presence of interlayers in a periodic structure optimized for maximum normal incidence reflectance, would only be about 4%. So, the effects of interlayers are more pronounced for wide bandpass multilayer structures. This can be explained by the fact that the thickness of absorbing layers (Mo) in an ideal structure can be varied over a wider range compared to a structure with 1 nm MoSi₂ interlayers. Once the interlayers are included, the absorber thickness cannot be lower than 2 nm (two 1 nm thick MoSi₂ interlayers with zero Mo layer thickness left). This fact limits degrees of freedom of optimization and, in particular, results in an increasing dispersion of the reflectivity curve.

In real life, the naturally formed interlayers cannot be fully controlled by the deposition technique. Their fine structure, i.e. the variation of density and atomic composition across interlayer, as well as the precise thicknesses are not known with the sufficient accuracy to realize the designed structures. One way to avoid this uncertainty is to introduce efficient diffusion barrier layers with known parameters that prevent the formation of natural interlayers. Below, we consider an example of artificial 1 nm Mo₂C diffusion barriers introduced at every boundary between Mo and Si. The stability of interfaces in a nonequilibrium Mo₂C-Si system is conditioned by the activation energy barrier that must be overcome to decompose Mo₂C and produce MoSi₂. In turn, the Mo₂C-Mo interface is rather stable, even at elevated temperatures, because this pair of materials are neighbors on the phase diagram and are in thermodynamic equilibrium with each other. The reflectivity and thermal stability of periodic Mo/Mo₂C/Si/Mo₂C multilayers have previously been experimentally studied in the EUV range [23]. The mean reflectivity of a Mo/Mo₂C/Si/Mo₂C mirror (sample 4 in Table 1) versus the target reflectivity is shown in Fig. 4 (curve 4), and the relative dispersion versus the mean reflectivity is presented in Fig. 6 (curve 4). The reflectivity of the mirror increases as the thickness of the barrier layers decreases. However, the technological difficulties involved in depositing ultra-thin layers along with the increased possibility of silicon and molybdenum diffusing through very thin Mo₂C films means that the thickness of the diffusion barriers cannot be too small.

The issue of interlayers can also be solved by selecting pairs of materials that form sharp interfaces. Following the example above, the entire Mo layer can be replaced by Mo₂C. Periodic Mo₂C/Si structures have been studied experimentally in the EUV range and it was suggested that no interlayers are formed in the system [23]. In our calculations, the structure is assumed to be free of interlayers (sample 5 in Table 1). With the same reflectivity dispersion, the Mo₂C/Si mirror has 2% higher reflectivity compared to the reflectivity of the Mo/Si mirror with interlayers. However, Mo-based multilayer mirrors with Mo₂C diffusion barriers will have better optical parameters than Mo₂C/Si mirrors because the optical constants of pure molybdenum are more suitable for multilayer mirrors operating at 13.5 nm.

3. Factors influencing the optical quality

In this section, we consider the effects of the number of bi-layers, minimum layer thickness limitations, inaccuracy of optical constants, interfacial roughness, and thickness errors, on

achievable optical parameters (plateau reflectivity, reflectivity dispersion) for depth-graded multilayer mirrors.

Let us consider the optical parameters of Mo/MoSi₂/Si/MoSi₂ mirrors with different numbers of bi-layers $N = 100$ and $N = 50$ (samples 2 and 3 in Table 1). Comparison of curves 2 and 3 in Fig. 4 show that mirrors with 50 bi-layers have almost the same reflectivity as mirrors with 100 bi-layers, i.e. the lower 50 bi-layers contribute minimally to the mean reflectivity. However, comparison between curves 2 and 3 in Figs. 3 and 4 show that, at a fixed value of dispersion, the mean reflectivity of the 100 bi-layer mirror is about 2% more than that of the mirror with 50 bi-layers. In other words, the lower 50 bi-layers, while not contributing to the mean reflectivity, smooth the reflectivity plateau.

Until now, we have discussed the results of calculations performed with the sole limitation that the layer thickness is a positive quantity. However, in some cases, the optimum thickness of the absorbing layers was found to be as small as 0.1-0.5 nm, which seems to be impractical to implement, as shown in Fig. 8 (filled symbols).

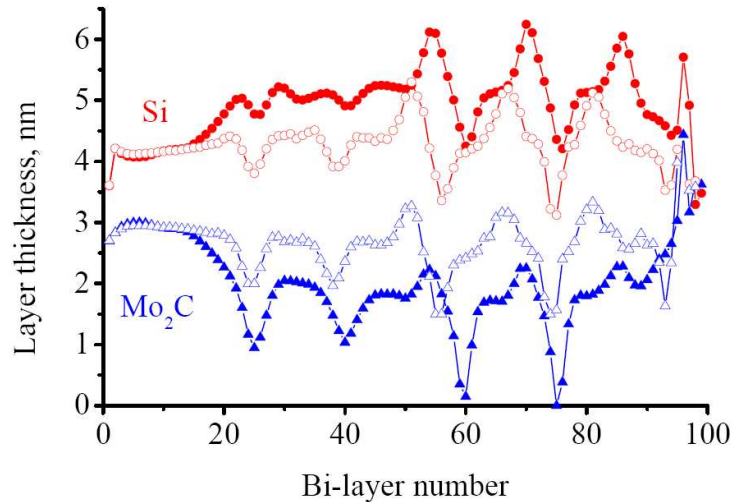


Fig. 8. The depth-distribution of the layer thickness for a Mo₂C/Si multilayer structure (sample 5 in Table 1), optimized for the average reflectivity $R_0 = 56\%$ in the $[0, 18^\circ]$ range of angle of incidence (filled symbols) and for a similar multilayer mirror with a limitation imposed on the thickness so that it is not less than 1.5 nm (unfilled symbols). Both designs result in virtually the same reflectivity profile.

To account for the technological constraints, we performed calculations such that a certain minimum layer thickness was required. Figure 9 shows the dependence of the relative dispersion of reflectivity on the minimum possible layer thickness for a Mo₂C/Si multilayer mirror. This shows that as the minimum layer thickness increases, the relative dispersion increases and, therefore, the greater the oscillations in the reflectivity curve. In the current case the relative dispersion increases dramatically when the minimum layer thickness exceeds 2 nm, because the constraint on the layer thickness limits the degrees of freedom of computer optimization of the structure. The depth-distribution of layer thickness calculated under the assumption of a 1.5 nm minimum layer thickness is shown in Fig. 8 (unfilled symbols). Although this solution of depth-distribution differs significantly from the solution without the imposed limitation, this design results in virtually the same reflectivity profile.

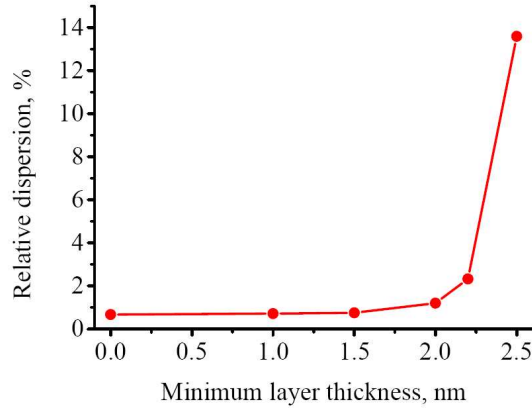


Fig. 9. The relative dispersion of the reflectivity versus the minimum possible layer thickness of the Mo₂C/Si multilayer mirror optimized for the average reflectivity $R_0 = 56\%$ in the $[0, 18^\circ]$ range of the angle of incidence.

The accuracy of the optical constants and, in particular, the density of materials used for calculations also influences the optical quality of depth-graded multilayer mirrors. Curve 1 in Fig. 10 shows the reflectivity profile of a Mo/MoSi₂/Si/MoSi₂ multilayer mirror designed with the assumption that the densities of all the materials are the same as their bulk densities. Curve 2 shows the reflectivity profile of the same mirror after the density of Mo has been reduced by 10%. This change results in a reduction of the reflectivity by 5% as well as increasing the distortion of the reflectivity curve (i.e. an increased RD value). On the other hand, the reflectivity is relatively unaffected by decreasing the density of Si or MoSi₂. This situation is identical to that of hard x-ray supermirrors, whose optical parameters are determined mainly by the polarizability of the absorbing layers [9]. Finally, curve 3 in Fig. 10 was calculated assuming the absorption of silicon to be 1.5 times higher than that given in the literature. Increasing absorption may be caused, for example, by impurities introduced during film deposition and, evidently this decreases the reflectivity with no significant distortion of the reflectivity curve.

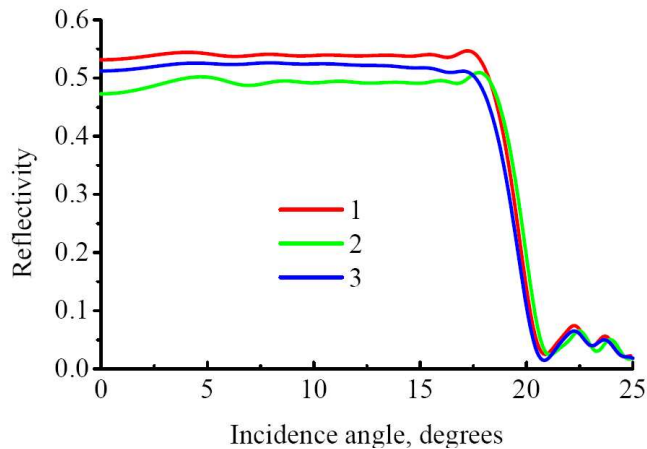


Fig. 10. The effect of layer density on depth-graded Mo/MoSi₂/Si/MoSi₂ multilayer mirror reflectivity (sample 2 in Table 1). Curve 1 is the result of optimization targeting $R_0 = 54\%$ and taking the density of all the layers to be the same as that of the bulk materials. Curve 2 is the reflectivity for the same layer thickness distribution but taking the density of Mo layers to be 0.9 of the bulk material density. Curve 3 was calculated taking the absorption of Si layers to be 1.5 times higher compared to the literature data.

Thus far, we have considered perfectly smooth multilayer structures. Now we will discuss the effect of interfacial roughness. We restrict ourselves to the following simplest cases: (a) totally conformal interfacial roughness with a large correlation length and (b) non-conformal interfacial roughness with a small correlation length. These two limiting cases contain the essential physics required for describing more complicated cases of interfacial roughness. The large-scale roughness is replicated during multilayer mirror deposition and, simultaneously, additional small-scale intrinsic roughness arises. In the first case, the decrease in the reflectivity is described by the Debye-Waller factor applied to the total reflectivity coefficient of the multilayer structure. In the second case, the decrease in the reflectivity is usually described by the Nevot-Croce factor applied to the amplitude reflectivity of each interface. The result of the calculations for interfacial roughness with a 0.3 nm rms height are shown in Fig. 11 for the conformal (curve 2) and the nonconformal (curve 3) cases. The effect of interfacial roughness is stronger for conformal roughness, which has a longer correlation length. Nevertheless, the even reflectivity plateau is still retained in both cases.

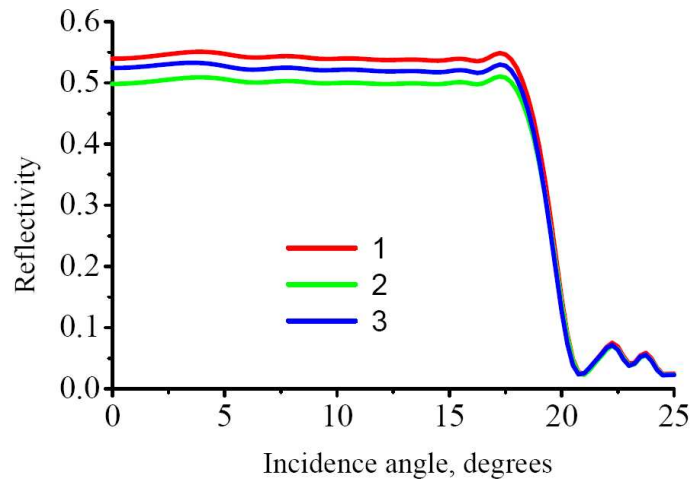


Fig. 11. The effect of interfacial roughness on the depth-graded Mo/MoSi₂/Si/MoSi₂ multilayer mirror reflectivity (sample 2 in Table 1). Curve 1 was calculated for $R_0 = 54\%$ with the assumption of perfectly smooth interfaces. Curves 2-3 were calculated for the same structure as curve 1 assuming 0.3 nm interfacial roughness. When calculating curve 2, the roughness of the different interfaces was supposed to be conformal and the correlation length large. In contrary, when calculating curve 3, the roughness was assumed to be nonconformal and the correlation length small.

Finally, we will discuss the effect of thickness errors. Thickness errors originate from imprecise thickness control, reaction fluctuations, or interdiffusion between adjacent layers. To estimate these effects, we consider two systems; Mo₂C/Si (no interlayers formed) and Mo/MoSi₂/Si/MoSi₂ (where MoSi₂ is a natural interlayer). Evenly distributed thickness errors, in the range of ± 0.05 nm, were included in our calculations and the results from five such calculations are presented here to show examples of possible effects on the reflectivity profile. In contrast to the factors discussed above, the random thickness errors resulted in a strong deformation of the reflectivity plateau (Fig. 12). The effect is more pronounced in the case of the Mo/MoSi₂/Si/MoSi₂ structure where the thicknesses of the interlayers were also subject to fluctuations.

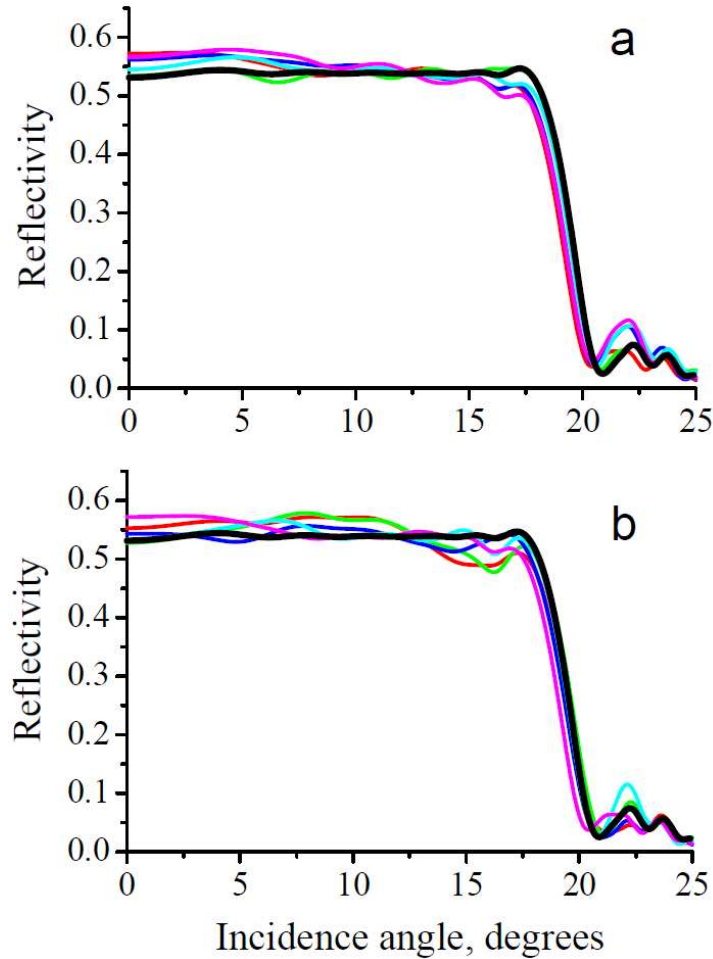


Fig. 12. (a) The reflectivity of a Mo₂C/Si multilayer mirror (sample 5 in Table 1) aimed at the constant reflectivity $R_0 = 54\%$ (black curve) as well as the reflectivity of the same multilayers with random layer thickness fluctuations evenly distributed in the ± 0.05 nm range (colored curves). Calculations were performed for five sequences of random layer fluctuations. (b) The same for the Mo/MoSi₂/Si/MoSi₂ multilayer mirror (sample 2 in Table 1).

This fact is explained by the cumulative effect of the random thickness fluctuations [24,25]. Indeed, layer thickness fluctuations result in a random shift of $(j + 1)$ th interface by the value $\Delta z_j = \sum_{i=1}^j \delta z_i$, where δz_i is the random fluctuation of i -th layer thickness and the summation is carried out over all the previous layers. Hence, the dispersion of the wave phase (DP_j) reflected from $(j + 1)$ th interface is proportional to the dispersion of the single layer thickness multiplied by the total number of previous layers: $DP_j \sim j \langle (\delta z)^2 \rangle$. The effect of the thickness errors becomes more pronounced for the Mo/MoSi₂/Si/MoSi₂ structures since they have double the number of layers for the same number of periods. Actually, in case of fixed interlayer thicknesses, the effect of thickness errors is very similar for Mo/MoSi₂/Si/MoSi₂ and Mo₂C/Si structures.

4. Pilot experiment

In our first pilot experiment, we designed and fabricated a depth-graded Mo/Si multilayer mirror for $\lambda = 13.5$ nm with a target reflectivity $R_0 = 60\%$ in the $[0, 16^\circ]$ range of the angle of incidence. The design consisted of 49.5 bi-layers, with silicon layers being placed on the top

and bottom of the structure. To account for the naturally formed interlayers, at every boundary between Mo and Si we introduced 0.8 nm thick interlayers consisting of a mixture of Mo_5Si_3 and MoSi_2 , as suggested by modelling of grazing incidence x-ray reflectivity, diffraction measurements and TEM of real e-beam deposited multilayers in our earlier work [18,26–28]. Finally the structure was covered with a 2 nm thick silicon oxide layer. The densities of all the layers were assumed to be the same as the densities of the bulk materials. We also assumed that each interface had 0.2 nm roughness with a very small correlation length in the plane of the interface. There is considered to be no correlation between the roughness of different interfaces throughout the stack. Therefore, the effect of the interface roughness was described by the Nevot-Croce factor applied to the amplitude reflectivity of each interface. The calculated depth-distribution of the Mo and Si layer thickness is presented in Fig. 13 (filled symbols) with the bi-layer number being counted from the top of the structure. Interlayers and the oxide layer are not shown in the figure. The target reflectivity profile is given by the green curve in Fig. 14. The designed depth-graded multilayer was deposited at one of the FOM coating facilities by means of e-beam evaporation and ion beam polishing [29–31], in an ultra high vacuum system (base pressure below 10^{-8} mbar). The growth of the layers was monitored by quartz mass balances and the roughness was reduced by Kr-ion polishing of the completed Si layers. The multilayer reflectance at near-normal incidence around 13.5 nm was measured at the Physikalisch Technische Bundesanstalt (PTB) [32,33] using the BESSY II storage ring in Berlin. The measured reflectance of the depth-graded multilayer versus the angle of incidence is shown in Fig. 14 (circles). The angular bandpass of reflection is close to the target value of 16° , demonstrating that the thickness profile is rather close to the intended one. However, the experimental reflectivity curve is deformed: the measured reflectivity is not constant at the plateau and varies between 50 to 60%. This fact, as well as an observed difference between the measured and the calculated reflectivity at larger angles, clearly demonstrates that the internal structure of the fabricated mirror differs somewhat from the designed one.

There are several factors that could lead to the observed deformation of the reflectivity curve. First of all, we note that the right part of the experimental reflectivity plateau (at $\varphi \sim 16^\circ$) is slightly shifted to the larger angles by about 0.6° as compared to the designed value. This shift can be caused, in accordance with the roughly applied Bragg law, by a systematic shift of all bi-layer thicknesses by a constant value of $\Delta d = d\Delta\varphi \cdot \tan\varphi \approx 0.021$ nm. One of possible reasons resulting in this inaccuracy is a slightly incorrect interlayer thickness used in the designing process. Unfortunately reflectometry data cannot resolve this uncertainty since it can only be done accurately for the periodic structures. At the same time this uncertainty also leads to the deformation of the reflectivity plateau at small incidence angle resulting in the observed 50 to 60% fluctuations.

A significant part of the shift and deformation of the reflectivity profile could also result from the uncertainty in the fine structure of the naturally formed interlayers, i.e. variation in the material density and its chemical composition across the interlayer, which is not known at the current state of research and, therefore, could not be taken into account in the design.

Finally the observed deviation of the experimental data could also be explained by the random layer fluctuations arising during deposition. The result of fitting the experimental reflectivity curve using random layer fluctuations while keeping the rest of the parameters the same as in the design is shown by the unfilled symbols in Fig. 13, and the corresponding reflectivity by the blue curve in Fig. 14. Note that the thickness distribution found by the optimization technique is not unique and there are a number of different thickness distributions that provide the same reflectivity profile within the prescribed accuracy. Nevertheless, Fig. 13 allows us to conclude that the deviation of the reflectivity curve could also be caused by small random deviations in the layer thicknesses.

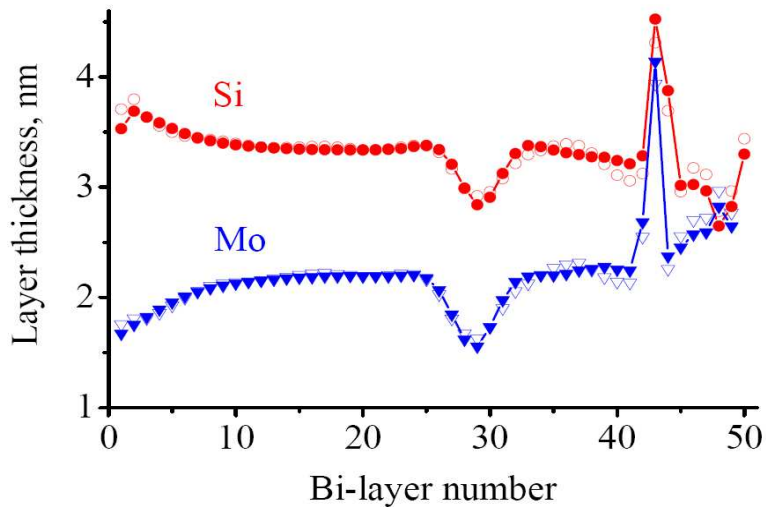


Fig. 13. The designed layer thickness distribution (filled symbols) of the Mo/Si multilayer structure ($N = 49.5$) targeting the constant reflectivity $R_0 = 60\%$ in the $[0, 16^\circ]$ range of the angle of incidence at $\lambda = 13.5$ nm. To account for the naturally formed interlayers 0.8 nm thick interlayers were introduced at every boundary between Mo and Si that are not shown at the graph. Unfilled symbols show the result of fitting to the experimental reflectivity curve.

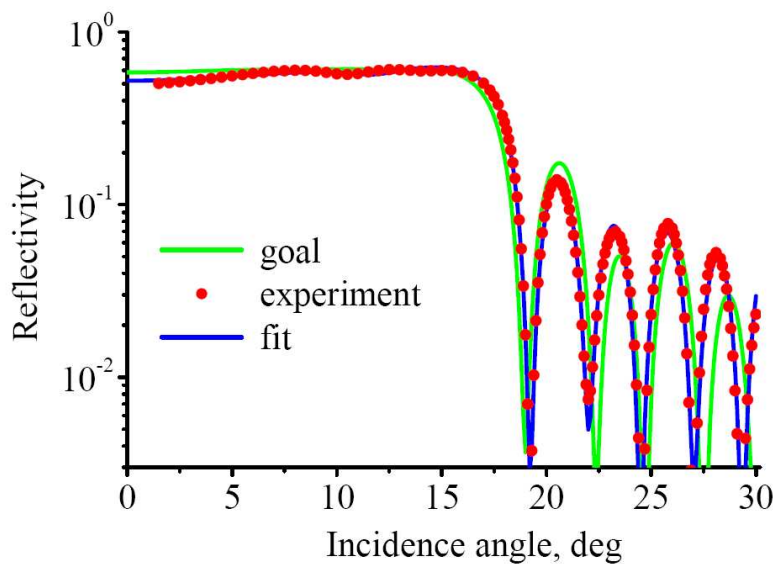


Fig. 14. The aimed (green curve) and the measured (red circles) reflectivity curve versus the angle of incidence (at $\lambda = 13.5$ nm) of the Mo/Si multilayer mirror aimed at the constant reflectivity in the $[0, 16^\circ]$ range of angle of incidence. Blue curve is the result of fitting allowing thickness fluctuations during deposition.

Therefore, the future improvement of the designing procedure implies the use of a more correct model of the naturally formed interlayers and designing multilayer structures with a reduced sensitivity to random layer thickness variations.

5. Conclusions

We theoretically analyzed the optical properties of multilayer mirrors with a wide angular bandpass in the EUV wavelength range and the factors that influence these properties. In general, a flat reflectivity profile cannot be achieved when an ideal stack is assumed during

the design stage. In particular, the formation of natural interlayers alters the reflectivity profile of Mo/Si systems considerably and, therefore must be taken into account during the design of the multilayer structure. Based on that, structures that do not form significant interlayers (e.g. Mo₂C/Si), or structures with stable and well controlled artificial barrier layers (e.g. Mo/Mo₂C/Si/Mo₂C), are preferable for practical applications. We have also shown that deviations in the thicknesses of individual layers play a crucial role in deforming the reflectivity plateau. The cumulative effect of these fluctuations on the reflectivity plateau make it preferable to design two-component mirrors that do not have significant interaction between the layers (e.g. Mo₂C/Si) rather than mirrors with diffusion barriers (e.g. Mo/Mo₂C/Si/Mo₂C) in spite of their somewhat lesser reflectivity.

We have successfully fabricated, by e-beam evaporation, a depth-graded Mo/Si multilayer mirror for the range [0, 16°] of angle of incidence for a wavelength of $\lambda = 13.5$ nm. However, the observed differences between the measured and the calculated reflectivity calls for further analysis. This should include thickness errors induced during deposition, as well as taking into account the fine structure of naturally formed interlayers.

Acknowledgements

This work is part of the FOM Industrial Partnership Programme I10 ('XMO') which is carried out under contract with Carl Zeiss SMT AG, Oberkochen and the 'Stichting voor Fundamenteel Onderzoek der Materie (FOM)', the latter being financially supported by the 'Nederlandse Organisatie voor Wetenschappelijk Onderzoek (NWO)' and the EC project more Moore carried under the coordination of ASML. All near normal reflectance measurements were performed at the Radiometry Laboratory of the Physikalisch Technische Bundesanstalt (PTB), Berlin (Germany). The authors also acknowledge the support of the ISTC (project #3124).